Fringe generation with non-uniformly coated long-period fiber gratings

Ignacio Del Villar[1], Francisco J. Arregui[1], Ignacio R. Matias[1], Andrea Cusano[2], Domenico Paladino[2], and Antonello Cutolo[2]

[1]*Departamento de Ingeniería Eléctrica y Electrónica, Universidad Pública de Navarra, 31006 Pamplona, Spain.*
[2]*Optoelectronic Division – Engineering Department, University of Sannio, C.so Garbaldi 107, 82100 Benevento, Italy*
parregui@unavarra.es

Abstract: In this work, the spectral characteristics of non-uniform symmetrically ring shaped coatings deposited on long-period fiber gratings (LPFGs) have been theoretically and experimentally investigated. To optimize the structure performances, the device was designed with a simulation tool based on vectorial analysis of modes in a multilayer cylindrical waveguide and coupled mode theory. Electrostatic self-assembling technique was selected to deposit with fine control uniform azimuthally symmetric coatings on the cladding of the LPFG. UV laser micromachining operating at 193nm was used to selectively remove the coating with high spatial resolution and with azimuthal symmetry. By locally and selectively removing portions of the overlay surrounding the LPFG from the middle of the grating, strong modifications of its spectral characteristics were observed. Phase-shift effects and multiple interference fringes have been observed for all the attenuation bands, strongly depending on the length of the uncoated region and the overlay features (thickness and optical properties). This provides a valid technological platform for the development of advanced photonic devices for sensing and telecommunication applications.

OCIS codes: (050.2770) Gratings, (060.2370) Fiber optics sensors, (120.2440) Filters, (140.2180) Excimer lasers, (260.2110) Electromagnetic theory, (310.1860) Deposition and fabrication.

References and Links

1. A. M. Vengsarkar, P. J. Lemaire, J. B. Judkins, V. Bathia, T. Erdogan and J. E. Spie, "Long-period fiber gratings as band rejection filters," J. Lightwave Technol. **14**, 58-65 (1996).
2. S. W. James and R. P. Tatam, "Optical fibre long-period grating sensors: characteristics and application," Meas. Sci. Technol. **14**, R49-R61 (2003).
3. J. R.Qiang and H. E. Chen, "Gain flattening fibre filters using phase shifted long period fibre grating," Electron. Lett. **34**, 1132-1133 (1998).
4. B. J. Eggleton, R. E. Slusher, J. B. Judkins, J. B. Stark and A. M. Vengsarkar, "All-optical switching in long period fiber gratings," Opt. Lett. **22**, 883-885 (1997).
5. K. W. Chung and S. Yin, "Analysis of widely tunable long-period grating by use of an ultrathin cladding layer and higher-order cladding mode coupling," Opt. Lett. **29**, 812-814 (2004).
6. M. N. Ng and K. S. Chiang, "Thermal effects on the transmission spectra of long-period fiber gratings," Opt. Commun. **208**, 321-327 (2002).
7. X. Chen, K. Zhou, L. Zhang, and I. Bennion, "Optical chemsensors utilizing long-period fiber gratings UV-inscribed in D-fiber with enhanced sensitivity through cladding etching," IEEE Photon. Technol. Lett. **16**, 1352-1354 (2004).
8. T. Allsop, M. Dubov, A. Martinez, F. Floreani, I. Khrushchev, D. J. Webb, and I. Bennion, "Long period grating directional bend sensor based on asymmetric index modification of cladding," Electron. Lett. **41**, 59-60 (2005).
9. L. Zhang, Y. Liu, L. Everall, J. A. R. Williams and I. Bennion, "Design and realization of long-period grating devices in conventional and high birefringence fibers and their novel applications as fiber-optic load sensors," IEEE J. Sel. Top. Quantum Electron. **5**, 1373-1378 (1999).

#80919 - $15.00 USD Received 9 Mar 2007; revised 13 Jun 2007; accepted 13 Jun 2007; published 13 Jul 2007

10. B. H. Lee and J. Nishii, "Bending sensitivity in-series long-period fiber gratings," Opt. Lett. **23**, 1624-1626 (1998).
11. T. Allsop, R. Reeves, D. J. Webb, I. Bennion and R. Neal, "A high sensitivity refractometer based upon a long period grating Mach-Zehnder interferometer," Rev. Sci. Instrum. **73**, 1702-1705 (2002).
12. Jin-Fei Ding, A. P. Zhang, Li-Yang Shao, Jin-Hua Yan, and Sailing He, "Fiber-taper seeded long-period grating pair as a highly sensitive refractive-index sensor," IEEE Photon. Technol. Lett. **17**, 1247-1249 (2005).
13. A. P. Zhang, Li-Yang Shao, Jin-Fei Ding, and Sailing He, "Sandwiched long-period gratings for simultaneous measurement of refractive index and temperature," IEEE Photon. Technol. Lett. **17**, 2397-2399 (2005).
14. I. Del Villar, M. Achaerandio, F. J. Arregui and I. R. Matias, "Generation of selective fringes with cascaded long-period fiber gratings," IEEE Photon. Technol. Lett. **18**, 1412 (2006).
15. R. Slavik, "Extremely deep long-period fiber gratings," IEEE Photon. Technol. Lett. 18, 1705-1707 (2006).
16. N. D. Rees, S. W. James, R. P. Tatam and G. J. Ashwell, "Optical fiber long-period gratings with Langmuir-Blodgett thin-film overlays," Opt. Lett. **27**, 686-688 (2002).
17. I. Del Villar, M. Achaerandio, I. R. Matias and F. J. Arregui, "Deposition of an Overlay with Electrostactic Self-Assembly Method in Long Period Fiber Gratings," Opt. Lett. **30**, 720-722 (2005).
18. A. Cusano, A. Iadicicco, P. Pilla, L. Contessa, S. Campopiano, A. Cutolo and M. Giordano, "Cladding mode reorganization in high-refractive-index-coated long-period gratings: effects on the refractive-index sensitivity," Opt. Lett. **30**, 2536-2538 (2005).
19. A. Cusano, P. Pilla, L. Contessa, A. Iadicicco, S. Campopiano, A. Cutolo, M. Giordano and G. Guerra, "High-sensitivity optical chemosensor based on coated long-period gratings for sub-ppm chemical detection in water," Appl. Phys. Lett. **87**, 234105 (2005).
20. Z. Y. Wang, J. R. Heflin, R. H. Stolen, S. Ramachandran, "Analysis of optical response of long period fiber gratings to nm-thick thin-film coatings," Opt. Express **13**, 2808-2813 (2005).
21. A. Cusano, A. Iadicicco, P. Pilla, L. Contessa, S. Campopiano, A. Cutolo, and M. Giordano, "Mode transition in high refractive index coated long period gratings," Opt. Express **14**, 19-34 (2006).
22. I. Del Villar, I. R. Matias and F. J. Arregui, "Deposition of coatings on long-period fiber gratings: tunnel effect analogy," Opt. Quantum Electron. **38**, 655-665 (2006).
23. D. W. Kim, Y. Zhang, K. L. Cooper and A. Wang, "Fibre-optic interferometric immuno-sensor using long period grating," Electron. Lett. **21**, 324-325 (2006).
24. Q. Chen, J. Lee, M. R. Lin, Y. Wang, S. S. Yin, Q. M. Zhang and K. A. Reichard "Investigation of tuning characteristics of electrically tunable long-period gratings with a precise four-layer model," J. Lightwave Technol. **24**, 2954-2962 (2006).
25. S. W. James, I. Ishaq, G. J. Ashwell and R. P. Tatam, "Cascaded long-period gratings with nanostructured coatings," Opt. Lett. **30**, 2197-2199 (2005).
26. E. Anemogiannis, E. N. Glytsis and T. K. Gaylord, "Transmission characteristics of long- period fiber gratings having arbitrary azimutal/radial refractive index variation," J. Lightwave Technol. **21**, 218-227 (2003).
27. T. Erdogan, "Fiber grating spectra," J. Lightwave Technol. **15**, 1277-1294 (1997).
28. G. W. Chern and L. A. Wang, "Transfer-matrix method based on perturbation expansion for periodic and quasi-periodic binary long-period gratings," J. Opt. Soc. Am. A **16**, 2675-2689 (1999).
29. G. Decher, "Fuzzy Nanoassemblies: toward layered polymeric multicomposites," Science **277**, 1232-1237, (1997).
30. F. J. Arregui, I. Latasa, I. R. Matías and R. O. Claus, "An optical fiber pH sensor based on the electrostatic self-assembly method," Proc. of the IEEE Sensors **1**, 107-110 (2003).
31. I. Del Villar, I. R. Matias, F. J. Arregui and M. Achaerandio, "Nanodeposition of materials with complex refractive index in long-period fiber gratings," J. Lightwave Technol. **23**, 4192-4199 (2005).
32. K. W. Chung and S. Yin, "Design of a phase-shifted long-period grating using the partial-etching technique," Microwave Opt. Technol. Lett. **45**, 18-21 (2005).
33. Y. Liu, J. A. R. Williams, L. Zhang and I. Bennion, "Phase shifted and cascaded long-period fiber gratings," Opt. Commun. **164**, 27-31 (1999).
34. S. Khaliq, S. W. James and R. P. Tatam "Fiber-optic liquid-level sensor using a long-period grating," Opt. Lett. **26**, 1224-1226 (2001)
35. I. Riant and F. Haller, "Study of the photosensitivity at 193 nm and comparison with photosensitivity at 240 nm influence of fiber tension: type IIa aging," J. Lightwave Technol. **15**, 1464-1469 (1997).

1. Introduction

Long-period fiber gratings (LPFGs) induce attenuation bands in the transmission spectrum based on the coupling between the core mode and the co-propagating cladding modes. Consequently, differently from fiber Bragg gratings (FBGs), where coupling between contra-propagating core modes occurs, LPFGs are strongly influenced by the surrounding medium

#80919 - $15.00 USD Received 9 Mar 2007; revised 13 Jun 2007; accepted 13 Jun 2007; published 13 Jul 2007

due to cladding modes coupling. Because of this, LPFGs have extended their applications to both optical communications and sensors fields [1-2]. In optical communications LPFGs are used as gain equalizers, optical switches and tunable filters [1,3-5], whereas in optical sensing they can measure strain, curvature, temperature and refractive index [2,6-9].

In view of the interesting properties of LPFGs, much research has been devoted to the improvement of these devices, mainly focused on the reduction of the width and the increase of the depth in the attenuation bands. In sensors field, many works have been developed to enhance the sensing capability of these in-fiber devices, such as Mach-Zehnder interferometers or cascaded LPFGs [10-12]. The introduction of finer-scale spectral features within the relatively broad attenuation bands is able to provide higher resolution in sensing measurement, leading also to the possibility to tailor the device spectral response for telecommunication applications, such as optical filters [13-14]. An additional contribution to the field of communications is the improvement in the depth of the attenuation band to more than 60 dBs [15].

Recently, symmetrically ring shaped high refractive index (HRI) coatings have been used with single or cascaded configurations [16-25]. The reason is their ability to induce a wavelength shift of the attenuation bands. This can be used for optical filter tuning in optical communications. But the most important property is that, for specific parameterization of the refractive index and the thickness of the coating, the sensitivity of the device can be improved by more than one scale order [21]. In particular, such structures, if adequately designed, show high sensitivity to the surrounding refractive index and to the coating features (refractive index and thickness). Moreover, if the coating is sensitive to a chemical species, the device can be used as a chemical sensor or a biosensor.

Based on this line of argument, we experimentally demonstrate in this work that phase shift effects and interference fringes generation involving all the attenuation bands can be easily obtained by using a single LPFG coated with non-uniform symmetrically ring shaped HRI coatings. In section 2 we show the design of the LPFG. For this design we use theoretical results obtained with a numerical method based on the vectorial analysis of modes and the application of coupled mode theory. In section 3, the methods for the deposition and the laser based selective stripping of the coating are presented. In section 4, the experimental results are presented and compared to those of section 2. The agreement between the experimental and theoretical results can be improved after including for the simulations of section 5 some factors not considered in section 2. To finish, some concluding remarks are offered in section 6.

2. LPFG design and fabrication

In LPFGs [see Fig. 1(a)] the modal coupling induces some attenuation bands in the transmission spectrum. Though the simple phase matching condition is sufficient to give an approximation of the central wavelength of the attenuation band, the modified phase matching condition is often preferred [26]:

$$\beta_{01}(\lambda)+s_0\zeta_{01,01}(\lambda)-\left(\beta_{0j}(\lambda)+s_0\zeta_{0j,0j}(\lambda)\right)=\frac{2\pi N}{\Lambda} \tag{1}$$

where β_{01} and β_{0j} are the propagation constants of the core and the j^{th} cladding mode respectively, $\varsigma_{01,01}$ and $\varsigma_{0j,0j}$ are the self-coupling coefficients of the core and the j^{th} cladding mode, s_0 is the coefficient of the first Fourier component of the grating, Λ is the pitch of the grating, and N is the diffraction order.

On the other hand, the depth of the attenuation band depends on the length of the grating L and the cross-coupling coefficient k_i between the core and the cladding mode [2]:

$$T_i=\cos^2\left(k_i L\right) \tag{2}$$

The optical fiber used in this work is a Fibercore PS 1250/1500 with a cut-off wavelength of 1155 nm and a numerical aperture of 0.14. The grating, of period 220 μm and of length

#80919 - $15.00 USD Received 9 Mar 2007; revised 13 Jun 2007; accepted 13 Jun 2007; published 13 Jul 2007

26.7 mm, was written with a point-by-point technique. The source used to this purpose was a 244-nm UV laser beam.

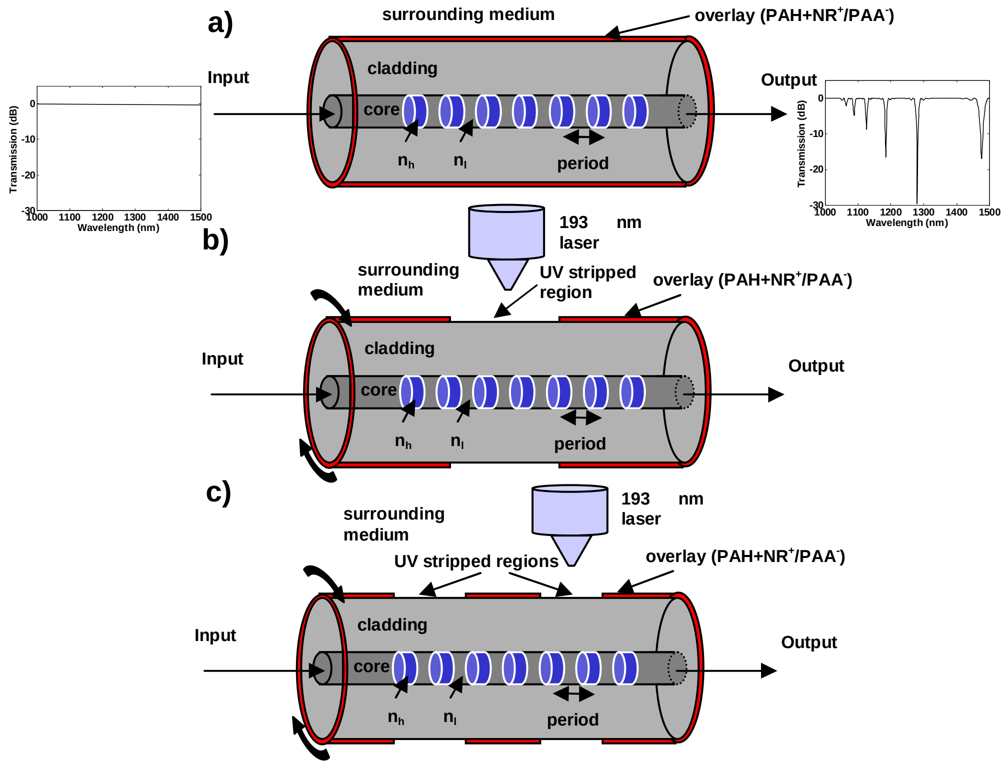

Fig. 1. Coated LPFGs: a) uniformly coated; b) coated with a middle stripped region; b) coated with two stripped regions

LPFGs are usually designed in such a way that the T_i approaches the value zero at the resonance wavelength [Eq. (1)]. Consequently, the depth of the attenuation band is maximum, which is adequate for filter applications in communications or for accurate detection of a parameter, if the device is used as an optical sensor. However, different attenuation band depths can be obtained depending of the product k_iL in Eq. (2). With a point-by-point irradiation technique it is easy to control the attenuation band depth. The cross-coupling coefficient k_i can be considered as constant, even though it can show a slow 'z' varying dependence [27]. As the grating length is increased it is obtained periodically minimum and maximum transmittivity in the attenuation band. In Fig. 2 it is represented the transmission spectra recorded for different grating lengths. For a grating of length 6.7 mm the product k_iL is $\pi/4$ (transmission -3 dB), for a grating of length 13.3 mm the product k_iL is $\pi/2$ (minimum transmission -30 dB), for a grating of length 20 mm the product k_iL is $3\pi/4$ (transmission -3 dB), and for a grating length of 26.7 mm the product k_iL is π (maximum transmission of 0 dB).

The value 26.7 mm is not randomly chosen. Previously to the inscription of the grating, it was numerically analyzed the effect of using different grating lengths in the generation of fringes in the transmission spectrum for non-uniformly coated LPFGs. The simulation method used is based on vectorial analysis of modes in a multilayer cylindrical waveguide and coupled mode theory [22]. The main novelty is the consideration of the mode coupling between different cylindrical waveguides [28] [see Figs. 1(b) and 1(c)].

#80919 - $15.00 USD Received 9 Mar 2007; revised 13 Jun 2007; accepted 13 Jun 2007; published 13 Jul 2007

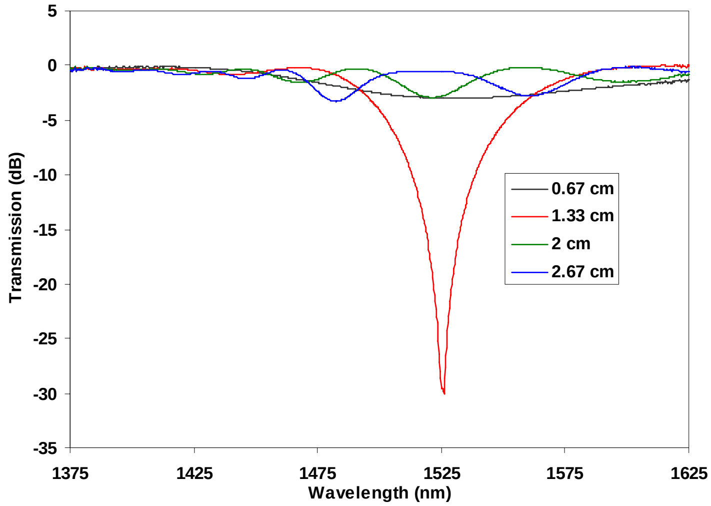

Fig. 2. Experimental transmission spectra as a function of the grating length of an LPFG

For two different grating lengths (13.3 mm and 26.7 mm) it will be analyzed the progressive stripping of the middle region (see Fig. 1(b)) of an LPFG where a coating has been deposited. In the experimental part of this work the LPFG is coated with electrostatic self-assembled polyallylamine hydrochloride and neutral red ($PAH+NR^{+}$) and polyacrylic acid (PAA^{-}) [29-30]. According to our estimations, the refractive index of these coatings is 1.54. We also consider the influence of scattering and roughness of the material as an additional imaginary refractive index of 0.005 [31]. The overlay thickness chosen is 300 nm. This value avoids the vanishing of the attenuation band [17] and guarantees a phase-shift between the modes and a consequent generation of fringes. The DC component and amplitude of the modulation in the core have been estimated 1.4709 and 4×10^{-4} respectively and the cladding refractive index 1.464708. For the sake of simplicity we will assume all the refractive indices constant in the wavelength range analyzed.

In Fig. 3(a) it can be visualized the effect of suppressing the middle region of the coating in a grating of 13.3 mm. In the spectrum analyzed there are two attenuation bands at 1190 nm and 1430 nm. As the middle region of the coating is stripped, the attenuation band depth decreases and two additional fringes are generated for each attenuation band. However, if the same analysis is done for a grating of 26.7 mm [Fig. 3(b)], the depth of the fringes is increased in a great manner. In particular, the middle fringe depth progressively increases until a specific stripping length, where it starts to decrease. As a result, a good design could be a stripped region of length 4 - 6 mm, which generates a maximum central fringe.

The explanation for the difference between the results of Fig. 3(a) and Fig. 3(b) it that the fringes generated by removing the coating of the LPFG belong to two optical regions inside the same device: the coated and the non-coated one. The depth of each fringe depends on the energy soaked by the region that generates the fringe. Because the optical path where the energy is soaked by the cladding is being shared by the two regions, the selection of a grating length that induces a maximum depth in the attenuation band (13.3 mm in Fig. 2) causes a progressive reduction of the fringe depth. With the design of Fig. 3(b) this problem is solved and it is possible to obtain a maximum depth in the fringes.

#80919 - $15.00 USD Received 9 Mar 2007; revised 13 Jun 2007; accepted 13 Jun 2007; published 13 Jul 2007

a)

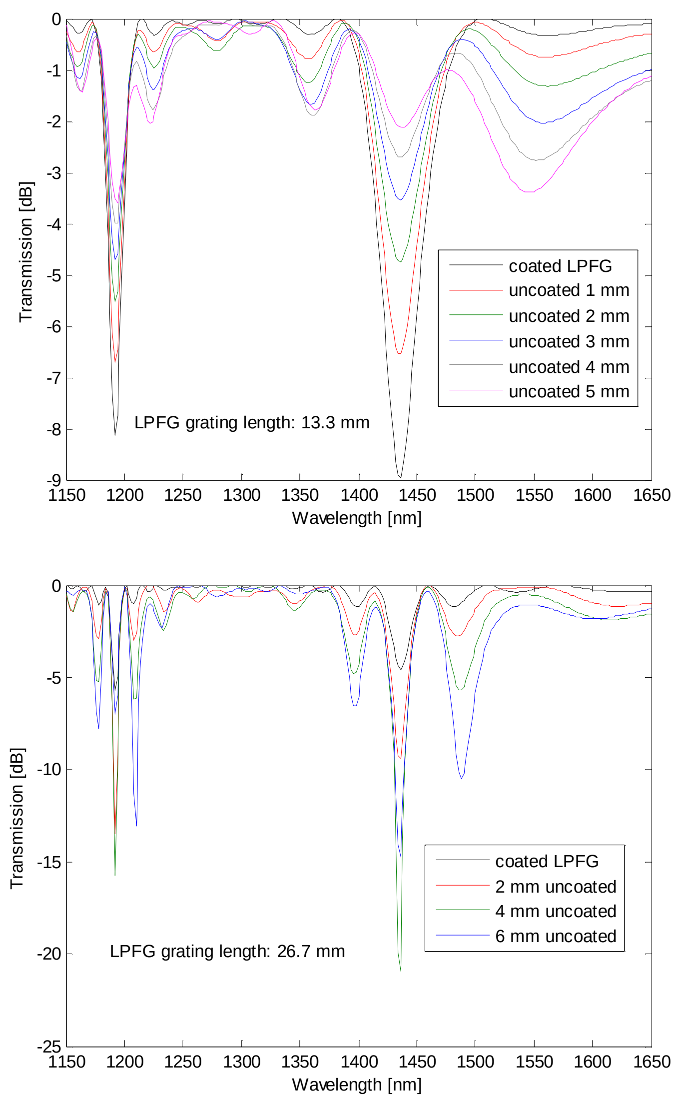

Fig. 3. Transmission spectra for coated LPFGs with different middle stripped regions for a) grating length 13.3 mm; b) grating length 26.7 mm

Note that the generation of fringes is not produced in the same manner as in phase-shifted LPFGs [32-33], where there is a substantial splitting of the attenuation band. In this case the central band maintains its features and, in particular, its spectral position. The generation of fringes is also possible with designs such as that of Fig. 1(c). In that case the fringes are generated by equally stripping two different regions with central points symmetrically placed at 6.7 mm from the middle of the grating of 26.7 mm. In Fig. 4 the transmission spectrum of such a structure is analyzed for different stripped lengths of each region. It is assumed that the coating is symmetrically stripped starting from the central points that we mentioned before. The maximum depth is obtained for stripped lengths between 5 mm and 8 mm. Since this last design does not induce the formation of more fringes than in Fig. 3, the simpler design of Fig. 1(b) will be used in the experimental part.

#80919 - $15.00 USD Received 9 Mar 2007; revised 13 Jun 2007; accepted 13 Jun 2007; published 13 Jul 2007

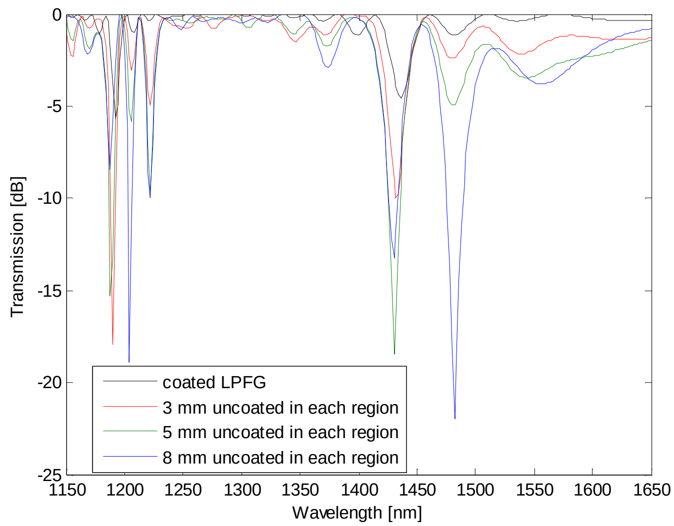

Fig. 4. Transmission spectra for coated LPFG with two stripped regions. The central point of the stripped regions is located at 6.7 mm from the grating center

3. Coating deposition and stripping procedure

The film deposition on the cladding of the LPFG is based on electrostatic self-assembly monolayer (ESAM) process [29]. This technique is based on the construction of molecular multi-layers by the electrostatic attraction between oppositely charged polyelectrolytes in each monolayer deposited, and involves several steps [29]. In the first step the substrate is immersed in a Piranha solution (a mixture of sulfuric acid and hydrogen peroxide) to create a charged surface. Since the substrate is, in this case, the optical fiber and the temperature may be close to 100 ºC it is necessary to provide a previous thermal treatment which adds stability to the attenuation bands. Otherwise there is a modification in the transmission spectrum each time that the LPFG is coated. The annealing procedure causes a reduction in the modulation index, which causes a slight increase in the attenuation band depth and a wavelength shift. This can be appreciated by comparing the spectrum of the LPFG of 26.7 mm in Fig. 2 with the spectrum of the uncoated LPFG of Fig. 5. Before the thermal treatment there is an attenuation band of 0 dB at 1525 nm (Fig. 2), whereas after the thermal treatment (Fig. 5) there is an attenuation band of 1 dB at 1470 nm. After that, the LPFG was coated with electrostatic self-assembled polyallylamine hydrochloride and neutral red ($PAH+NR^+$) and polyacrylic acid (PAA^-). In Fig. 5 it is also represented the final spectrum after deposition of the 300 nm thin coating. In order to capture the transmission spectra the grating was illuminated from one side with a broadband light source Agilent 83437A and the transmitted light was captured with an optical spectrum analyzer Agilent 86140B.

Once the LPFG is uniformly coated, a local and selective removal of the overlay was carried out to create non-uniform coatings along the grating. To this aim, an argon fluoride (ArF, λ = 193 nm) excimer laser merged with a dedicated equipment was used. The laser system is based on the principle of the mask image projection (masks of different shapes and dimensions are available) and it is completely computer-aided. In order to work on optical fibers, an automated rotating stage (see Fig. 6) is positioned under the laser firing point. It consists of two motorized mandrels to host the fiber. This component is capable to rotate the sample in both directions with selectable rotation angle and rotation speed. Its main peculiarity is the possibility to develop ring shaped micro-fabrications, combining the firing process with a rotation operation with proper characteristics. After the insertion of the LPFG in the rotating stage the terminations of the optical fiber containing the LPFG are forced to

#80919 - $15.00 USD Received 9 Mar 2007; revised 13 Jun 2007; accepted 13 Jun 2007; published 13 Jul 2007

pass over small pulleys (shown in the left and right hand sides of Fig. 6). In order to stretch the structure in a repeatable manner two masses of about 20 g are fixed at the terminations. In this way, the movements of the target and the firing process are performed under conditions of constant strain over the grating. During the stripping procedure a fiber rotation speed of 10 °/s and a laser repetition rate of 10 Hz with a fluence of approximately 25 mJ/cm^2 were chosen in order to remove the polymeric coating and keep also the laser power under the glass ablation threshold.

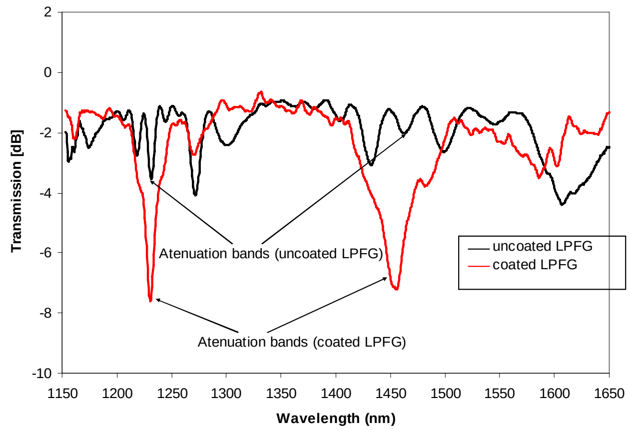

Fig. 5. Transmission spectrum of the LPFG before and after the coating deposition

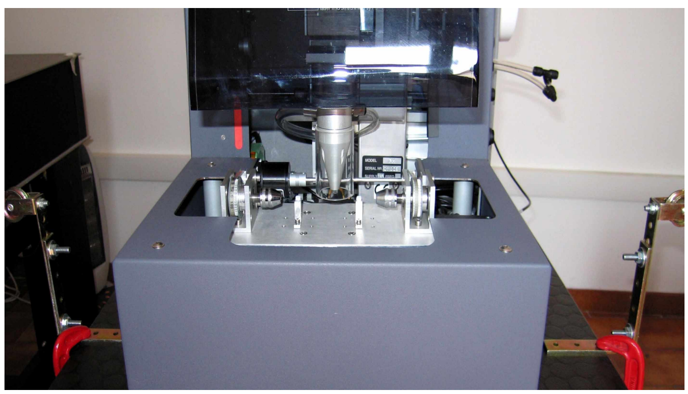

Fig. 6. Excimer laser system with rotating stage equipment

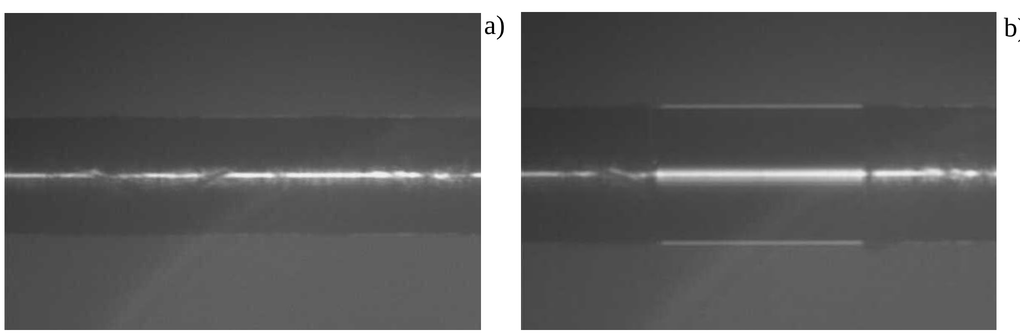

Fig. 7. Image through the laser vision system of coated LPFG: (a) section of the completely coated structure; (b) 200µm stripped coating

#80919 - $15.00 USD Received 9 Mar 2007; revised 13 Jun 2007; accepted 13 Jun 2007; published 13 Jul 2007

Figure 7 proves that, working with the aforementioned parameters of the laser system, it is possible to completely remove the deposited overlay from the LPFG. The images are from the vision system of the laser machine. Figure 7(a) reported a picture of the completely coated structure. The presence of the coating layer darkens the typical brightness characterizing the aspect of the glass structure through the laser vision system. In Fig. 7(b) the brightness of the structure corresponding to the fired area points out the selective disappearance of the coating layer for a longitudinal length of 200 μm. Note that the boundaries of the stripped region are well-defined by the presence of the coating on the two sides. Moreover no defects are evident all along the fired region: this means that the firing process preserves the glass structure.

4. Experimental results

The selective stripping procedure starts from the middle of the selected LPFG, removing the overlay for a longitudinal length of 100μm during each step. The uncoated region is thus progressively enlarged in successive steps, maintaining the symmetry of the structure with regard to the middle of the grating. Because of this, it is possible to individuate two lateral coated regions of identical length and a central uncoated area along the LPFG. As the central region progressively widens itself, the lateral ones decrease in length. The laser firing process is repeated until the complete stripping of the coating along the LPFG is achieved.

The progressive stripping induces strong modifications on the grating spectral response as shown in Fig. 8(a). The changes in the attenuation bands located at 1230 nm and 1450 nm for stripped region lengths of 2.8 mm and 5.3 mm, respectively, are reported. The spectra are compared to the uniform coating case. While the stripping process goes on, a progressive splitting of both the attenuation bands has been observed, which does not agree with the theoretical results of section 2, where no band splitting was predicted. On the other hand the experimental results are very similar to those exhibited by phase-shift LPFGs [32-33]. The reason is the presence of an additional phenomenon that is discussed at the end of this section.

In order to understand the reasons for band splitting formation within the transmission spectrum of the device, the theory of phase shift in periodic structure can be used.

In the investigated structure, in fact, a distributed phase-shift is generated by the mismatch in the effective refractive indices of the cladding modes between uncoated and coated regions, respectively. This phase-shift Φ can be expressed as follows [32]:

$$\Phi = \frac{2\pi}{\lambda} \cdot \Delta n_{eff,clad} \cdot L_{strip} \tag{3}$$

where $\Delta n_{eff,clad}$ is the refractive index difference of the cladding modes between the unperturbed and perturbed regions, L_{strip} the stripped length and λ the optical wavelength .

The amount of the phase delay is, thus, ruled by the overlay features (thickness and refractive index) and by the stripped length.

A perfect matching of peaks amplitude, corresponding to a phase-shift of π, is reached for an uncoated region lengths of 2.7 mm and 2.9 mm for the attenuation bands at 1230 nm and 1450 nm respectively. This is logical since, as reported in Eq. (3), the phase-shift inversely depends on the optical wavelength, leading to a higher phase-shift at lower wavelengths for a given overlay and stripped length. Rigorously, however, in the last calculation also the dependence of the effective refractive index changes between coated and uncoated regions on the mode order should be taken into account. By further increasing the uncoated region length, the side-attenuation bands at higher wavelengths completely disappear while the other ones exhibit an attenuation approaching the value of 14 dB for the 1230 band and 12 dB for the 1450 band in correspondence of a stripping length of 5.3 mm. This value should correspond to a phase-shift of approximately 2π for both the attenuation bands. The phase-shift phenomenon repeats as the uncoated length is increased, showing a quasi-periodic behavior [ee Fig. 8(b)]. The obtained results clearly recall the operating principle of phase-shift based devices, where the splitting phenomenon repeats as the phase-shift exceed 2π.

#80919 - $15.00 USD Received 9 Mar 2007; revised 13 Jun 2007; accepted 13 Jun 2007; published 13 Jul 2007

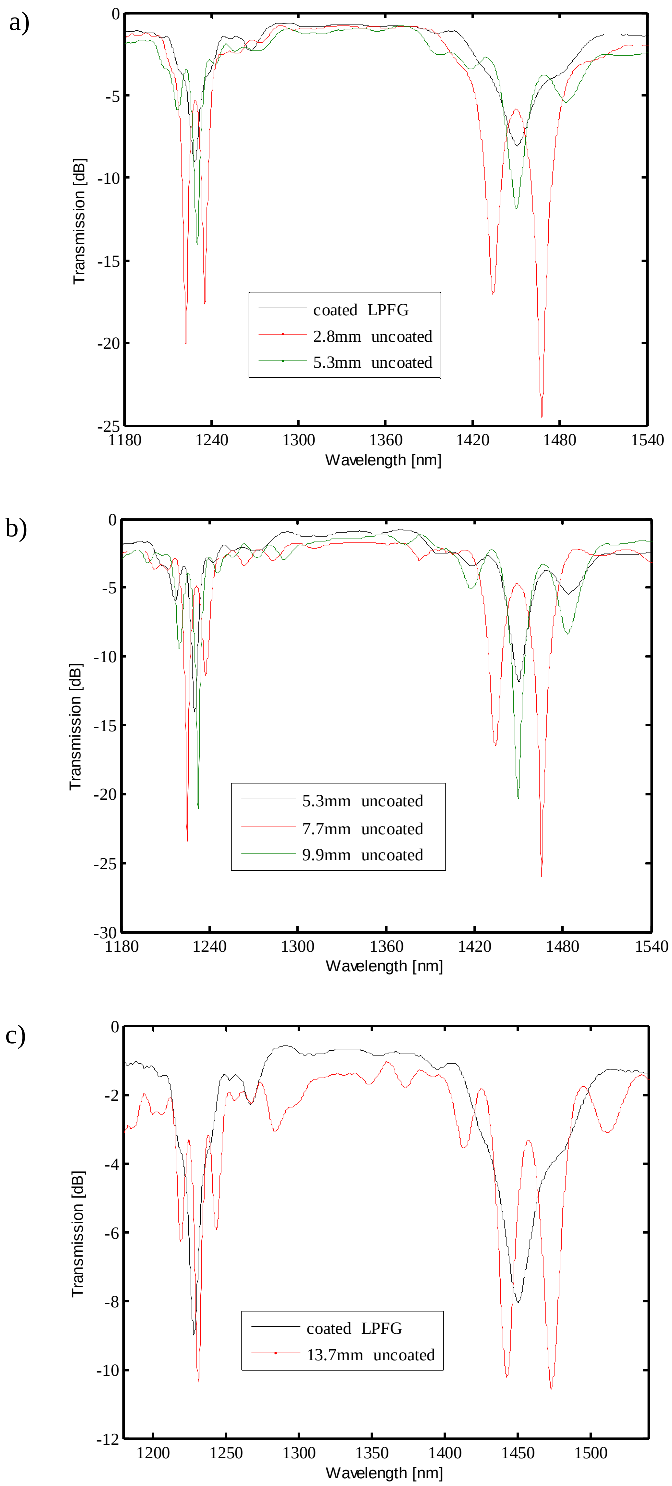

Fig. 8. Experimental transmission spectra during the first coating stripping: (a) phase-shift phenomenon in the range 0 - 2π; (b) phase-shift phenomenon in the range 2π - 4π; (c) multiple fringes generation

#80919 - $15.00 USD Received 9 Mar 2007; revised 13 Jun 2007; accepted 13 Jun 2007; published 13 Jul 2007

However, by increasing the uncoated length, the phenomenon can be no longer modeled as a pure phase-shift effect. In fact, the uncoated grating part, as the stripping length is increased, can not be regarded as a simple phase delay segment, since its attenuation bands begin to be relevant, playing a not negligible role in the modes beating. Figure 8(c) shows the spectral evolution of the attenuation bands as the uncoated region is remarkably increased: the effect of multiple interference fringes is now evident. This phenomenon is analogous to the increase in the number of fringes as the separation between two 3dB gratings is increased except for the fact that in this case there are three gratings involved in the band beating [33]. This means that, as the uncoated length approaches the coated ones, beating between the modes of the three grating regions occurs. As a result, there is a generation of interference fringes, which can be controlled by acting on the stripped length and/or on the coating features.

The stripping process was stopped when the coating was completely removed from the grating structure. However, the device spectrum after the coating removal was found different from the original one (see black curve in Fig. 9). Differently from the black curve in Fig. 5, now the grating presents three well-defined attenuation bands located at approximately 1180 nm, 1300 nm and over 1650 nm, with depth of about 5 dB, 6 dB and 10 dB, respectively. This means that also the effects of the laser radiation on the grating features should be taken into account. This is the reason why there is mismatch between numerical results of Fig 3(b) and the experimental results of Fig. 8 as demonstrated in the following. In Ref. [35], the photosensitivity in germano-silicate fibers at 193nm is studied and the writing of FBGs with fluence values of about 110 mJ/cm^2 is demonstrated. In this case, the laser fluence is limited to 25 mJ/cm^2. However, the LPFG was written in boron co-doped optical fiber.

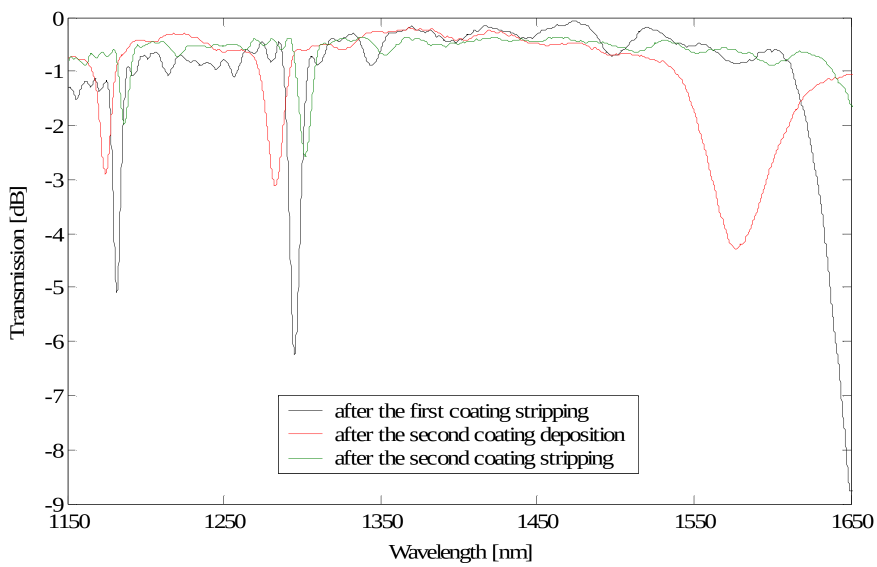

Fig. 9. Transmission spectrum of the LPFG after the first coating stripping, after the second coating deposition and after the second coating stripping

In order to better understand the effects of the laser firing, the grating has been re-coated with the same 300 nm thick overlay. According to the uniformly HRI coated LPFGs theory [21], such a coating induces a blue shift in the spectral position of all the original attenuation bands (see red curve in Fig. 9). In particular blue shifts of about 8 nm and 12 nm have been observed for the attenuation bands at 1180 nm and 1300 nm respectively. A second laser processing has been carried out uniformly along the grating, following the same sequence of steps of the first laser stripping.

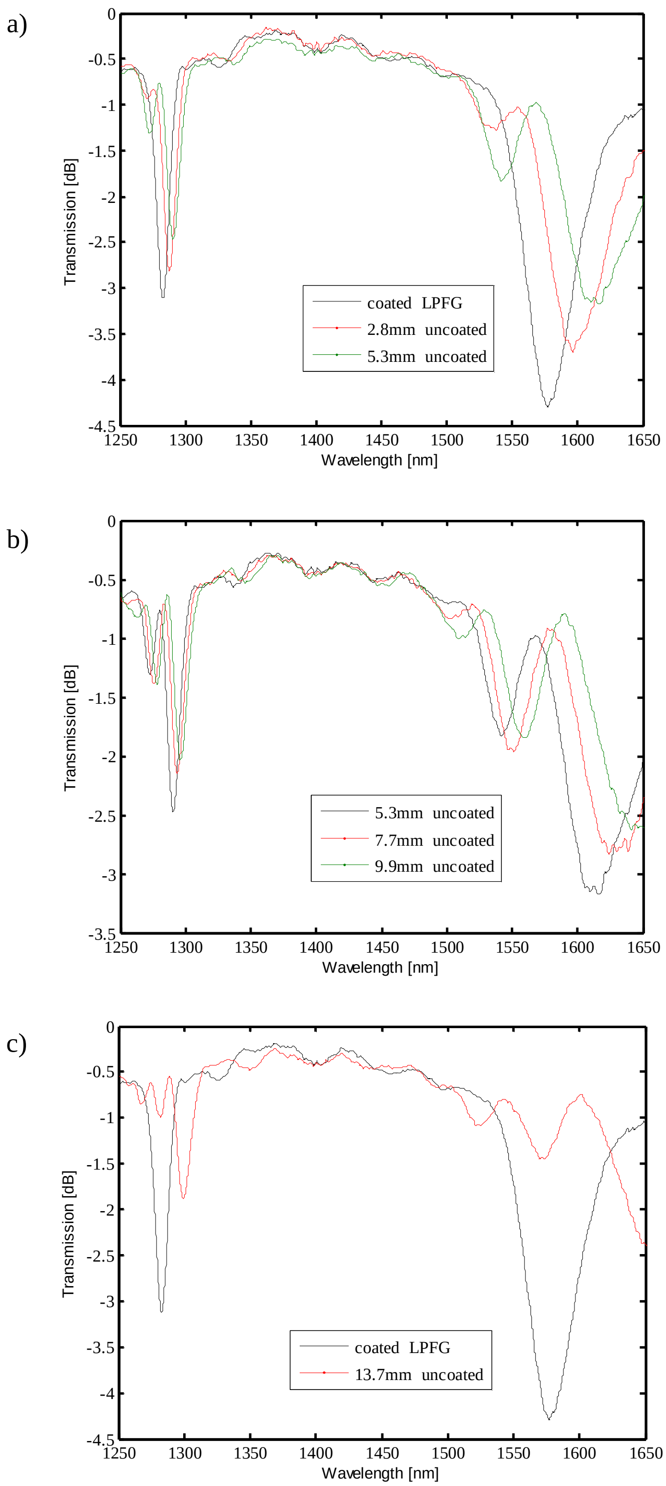

Fig. 10. Experimental transmission spectra during the second coating stripping. The same stripping lengths of Fig. 8 have been considered

#80919 - $15.00 USD Received 9 Mar 2007; revised 13 Jun 2007; accepted 13 Jun 2007; published 13 Jul 2007

By analyzing Fig. 9, two important differences have been observed comparing the LPFG spectrum before the second coating deposition and after its removal: the attenuation bands demonstrated red shifts (5 nm and 7 nm for the 1180 nm and 1300 nm attenuation bands, respectively) and a decrease in depth (of approximately 2 dB and 3.5 dB, respectively). Considering the modal coupling theory along LPFGs [27], both these spectral modifications could be motivated by the uniform laser radiation on the local core refractive index. In particular, the wavelength shift could be associated to an increase in the core index average value and the depth decrease to a diminution of the core modulation depth. Possible modifications on the cladding refractive index can be considered negligible if compared to the UV induced core refractive index changes.

The fringes generation during the second coating stripping can be appreciated in Fig. 10. Phase-shift effects or multiple fringes generation can be still observed in dependence of the stripped length, but, in this case, the effects of the first laser radiation cause a different spectral evolution. In particular, as observable from Figs. 10(a) and 10(b), π phase-shift condition, corresponding to a perfect matching of the two peaks, has never been reached. More generally, due to the diminution of the attenuation band depth, it is more difficult to appreciate the same effects observed during the first stripping procedure.

5. Theoretical results

In order to validate the conjecture of the previous section, the theoretical analysis of section 2 has been opportunely modified taking into account the laser effects. Note that, previously, the fiber was locally irradiated with a 244 nm laser for grating writing: a local increase of the core index was induced in correspondence of the irradiated regions. During the stripping procedure, instead, the LPFG can be considered as uniformly irradiated by the 193 nm laser. Those regions that were not attacked during the grating writing will experiment a more important refractive index variation during the stripping process. The result is a modification of the DC and the first Fourier component of the grating profile. Considering Fig. 11, it can be concluded that the DC component increases and the first Fourier component decreases. According to the conjecture of section 4, the increase in the DC component is responsible for a red shift of the original attenuation band after the laser stripping, whereas the decrease in the first Fourier component causes a modification in the depth of the attenuation band.

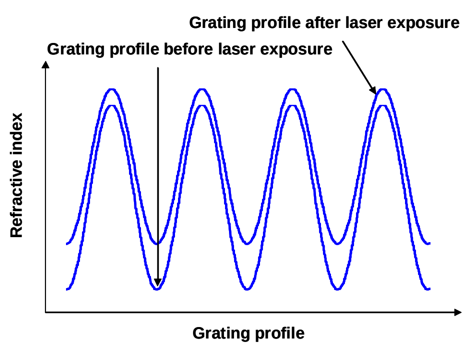

Fig. 11. Grating profile before and after 193 nm laser exposure

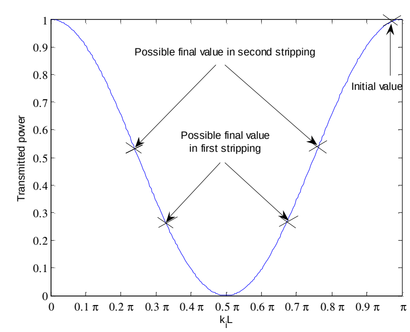

Fig. 12. Transmitted power as a function of $k_i L$

In Fig. 12 it is represented the evolution of the transmitted power as function of $k_i L$. It is departed from an initial state where the transmission is nearly 1 (0 dB). After impinging on fiber with the laser, the k_i (it is a function of the index modulation) was progressively reduced. By observing that the depth of the attenuation band after stripping the LPFG was about 6 dB (25% of transmitted power) we must be at one of the two points marked for the final value after first stripping in Fig. 12.

#80919 - $15.00 USD Received 9 Mar 2007; revised 13 Jun 2007; accepted 13 Jun 2007; published 13 Jul 2007

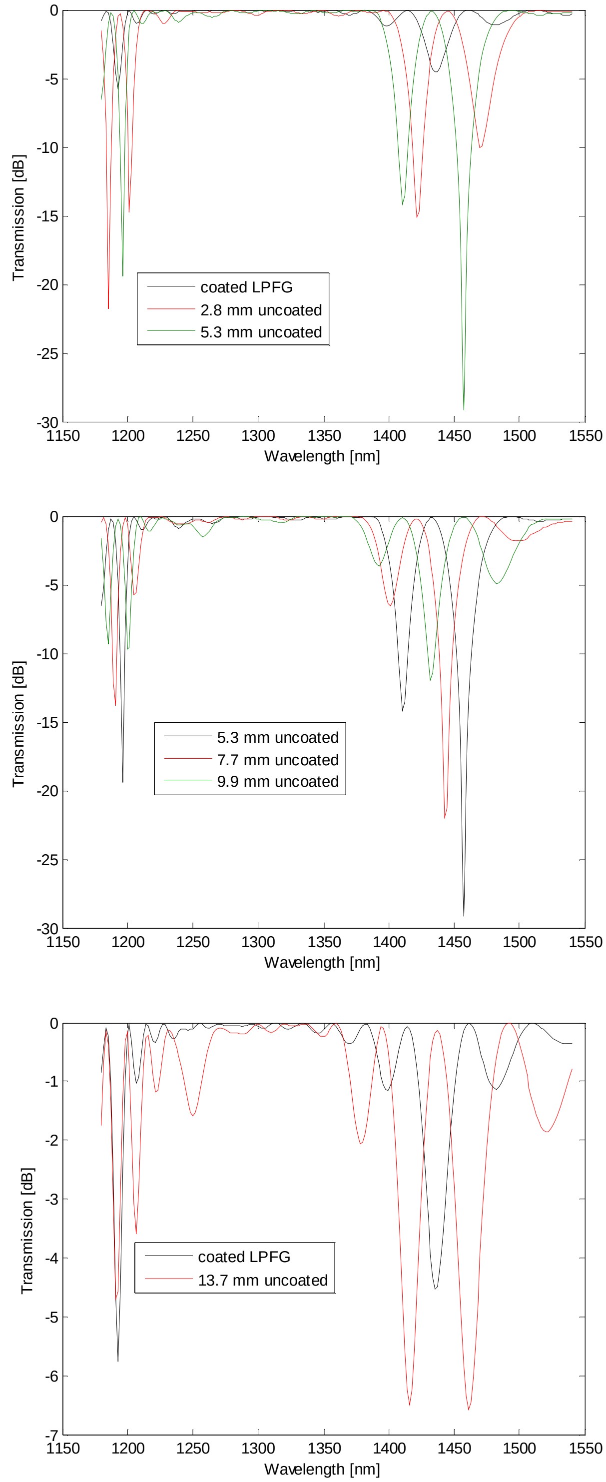

Fig. 13. Numerical transmission spectra during the first coating stripping taking into account the laser effects: (a-b) phase shift phenomenon in the range 0 - 4π; (c) multiple fringes generation

#80919 - $15.00 USD Received 9 Mar 2007; revised 13 Jun 2007; accepted 13 Jun 2007; published 13 Jul 2007

To summarize: the initial value is $k_iL \cong \pi$, and the final value in the first stripping must be either $k_iL \cong 0.32\pi$ or $k_iL \cong 0.68\pi$. In the second stripping the attenuation band depth is about 3dBs (50% of transmitted power). Again there are two possibilities: $k_iL \cong 0.22\pi$ or $k_iL \cong 0.78\pi$. Of these possibilities the only true one is $k_iL \cong 0.22\pi$, because the other one means the laser induces an increase in the modulation depth, which is not the case in Fig. 11. This also permits to discard the solution $k_iL=0.68\pi$ in the first stripping, because this would mean that in the second stripping the modification in the index modulation is higher than in the first one.

The parameters introduced for the DC component and amplitude of the modulation index before the LPFG was irradiated with the 193 nm laser were 1.4709 and 4×10^{-4}. After the first exposure it is considered that both parameters are 1.471115 and 1.5×10^{-4} respectively. The results of the simulations are presented in Fig. 13. In contrast to section 2, now both phase-shift phenomenon and multiple fringes generation are observable. The results corroborate the experimental ones of section 4. However, experimental and numerical phase-shifts do not occur for the same stripped lengths due to errors made in the parameterization introduced in the numerical analysis. In Fig. 13(a), the π phase-shift is obtained between 2.8 mm and 5.3 mm. In Fig. 13(b) the 2π phase-shift is obtained at about 9.9 mm, unlike in Fig. 8(a), where the 2π phase-shift was obtained for 5.3 mm. Finally, in Fig. 13(c) it can be visualized the multiple fringes generation, which agrees with that obtained in Fig. 8(c).

6. Conclusions

In conclusion, in this work, we demonstrated how by depositing non-uniform symmetrically ring shaped coatings on LPFGs it is possible to generate interesting and tailorable spectral features such as phase-shift behavior and multiple interference fringes operation, depending on the overlay features (geometry, refractive index and thickness). A proper experimental setup was implemented to fabricate the proposed devices, involving electrostatic self-assembly technique for coating deposition and an UV laser micromachining tool, specifically designed to produce non-uniform coatings with controlled geometry and azimuthal symmetry.

The LPFG was initially designed aided by a simulation tool based on vectorial analysis of modes in a multilayer cylindrical waveguide and coupled mode theory. Maximum fringe generation was observed for a grating of double length than the typical values used for communications and sensor fields. It was also predicted that no phase-shift phenomenon should occur. However, after the experiments both phase-shift phenomenon and multiple fringes generation were observed. The cause is that the laser used for stripping the coating induces a modification in the core refractive index of the boron co-doped fiber used for the experiments. After considering the effect of the laser in the simulations, there is a better agreement between the experimental and the theoretical results. In order to avoid this issue non-photosensitive fibers such as hydrogen loaded ones should be used for the experiments,

The exhibited functionalities extend the capabilities of LPFG based devices, enabling the development of new photonic components for sensing and telecommunication applications.

Acknowledgments

This work was supported by Spanish Ministerio de Educacion y Ciencia and FEDER Research Grants CICYT-TIC 2004-05936-C02-01/MIC and TEC 2006-12170/MIC.

#80919 - $15.00 USD Received 9 Mar 2007; revised 13 Jun 2007; accepted 13 Jun 2007; published 13 Jul 2007